

Adaptive Control of Soft Robots Based on an Enhanced 3D Augmented Rigid Robot Matching

Trumic, Maja; Della Santina, Cosimo; Jovanovic, Kosta; Fagiolini, Adriano

DOI

[10.23919/ACC50511.2021.9482817](https://doi.org/10.23919/ACC50511.2021.9482817)

Publication date

2021

Document Version

Final published version

Published in

Proceedings of the 2021 American Control Conference, ACC 2021

Citation (APA)

Trumic, M., Della Santina, C., Jovanovic, K., & Fagiolini, A. (2021). Adaptive Control of Soft Robots Based on an Enhanced 3D Augmented Rigid Robot Matching. In *Proceedings of the 2021 American Control Conference, ACC 2021* (pp. 4991-4996). IEEE. <https://doi.org/10.23919/ACC50511.2021.9482817>

Important note

To cite this publication, please use the final published version (if applicable).
Please check the document version above.

Copyright

Other than for strictly personal use, it is not permitted to download, forward or distribute the text or part of it, without the consent of the author(s) and/or copyright holder(s), unless the work is under an open content license such as Creative Commons.

Takedown policy

Please contact us and provide details if you believe this document breaches copyrights.
We will remove access to the work immediately and investigate your claim.

Green Open Access added to TU Delft Institutional Repository

'You share, we take care!' - Taverne project

<https://www.openaccess.nl/en/you-share-we-take-care>

Otherwise as indicated in the copyright section: the publisher is the copyright holder of this work and the author uses the Dutch legislation to make this work public.

Adaptive Control of Soft Robots Based on an Enhanced 3D Augmented Rigid Robot Matching

Maja Trumić^{1,2}, Cosimo Della Santina^{3,4,5}, Kosta Jovanović², Adriano Fagiolini¹

Abstract—Despite having proven successful in generating precise motions under dynamic conditions in highly deformable soft-bodied robots, model based techniques are also prone to robustness issues connected to the intrinsic uncertain nature of the dynamics of these systems. This letter aims at tackling this challenge, by extending the augmented rigid robot formulation to a stable representation of three dimensional motions of soft robots, under Piecewise Constant Curvature hypothesis. In turn, the equivalence between soft-bodied and rigid robots permits to derive effective adaptive controllers for soft-bodied robots, achieving perfect posture regulation under considerable errors in the knowledge of system parameters. The effectiveness of the proposed control design is demonstrated through extensive simulations.

Index Terms—robotics, flexible structures, adaptive control, modeling, uncertain systems

I. INTRODUCTION

BEING endowed with morphological flexibility and compliance, continuum soft robots promise to have a disruptive impact in several areas where safety, robustness, and adaptability are a main concern [1]. Yet, to fully exploit their potentialities, one has to face the challenge of dealing with systems characterized by states of theoretically infinite sizes. One possible strategy to deal with such systems is by using model-free machine learning techniques that regard a soft robot as a black box [2]. On the other end of the spectrum, model-based techniques fully taking into account the infinite nature of the problem are still unfeasible [3].

These reasons have steered the research attention towards the development of approximated but finite-dimensional models [4], [5], trading modeling accuracy with numerical efficiency, as well as reduced-order models, enabling an analytic design of model-based controllers [6]. Within this context, the Piecewise Constant Curvature (PCC) approximation-based paradigm is an effective attempt to leverage on the equivalence between a soft-bodied robot and a large enough rigid one via a suitable augmented formulation, aiming at enabling a variety of classical control approaches already established in robotics. The PCC approach is nowadays an established technique in

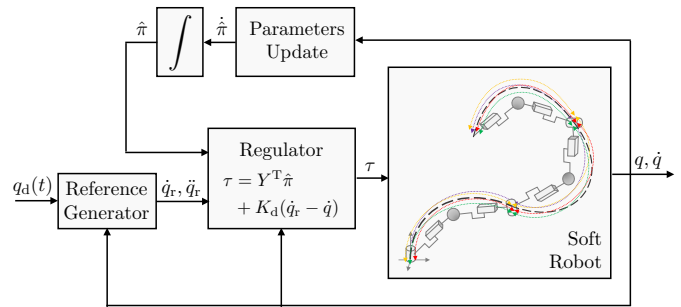


Fig. 1. Block scheme of the control algorithm introduced in this work. The soft robot with piecewise constant curvature is matched to a dynamically equivalent augmented rigid robot. This model is then used to derive an adaptive controller able to implement trajectory tracking in configuration space without the knowledge of any of the soft robot physical parameters.

kinematic control of continuum soft robots [7]. More recently, it has been proven to be effective also for open loop dynamic control [8]. A step further has been done in [9], [10] where the PCC dynamics has been connected with the one of a rigid robot subject to a set of embeddable holonomic constraints. In this way, model-based feedback controllers developed for rigid robots could be easily extended to the PCC case. The planar case is discussed in [9] while the three dimensional case is addressed in [10]. However, this latter work relies on the classic 3D representation of PCC robots [7], which is subject to several singularities issues making the controller not well defined in several boundary conditions (e.g. straight configuration). In [11], we discuss that these issues can be solved by using a different parameterization of the configuration manifold of a PCC robot, which is global and everywhere well defined. However, no connection to the augmented rigid robot formulation is provided in that work. A first contribution of the present work is therefore to extend the 3D augmented rigid representation of [10] to the improved parameterization proposed in [11]. By capitalizing on the advantages of [10] and [11], the paper describes a new parameterization overcoming singularity and discontinuity issues, while also establishing a link between soft-bodied and rigid-bodied robots by means of the augmented formulation. This connection is instrumental to the derivation of controllers which are numerically stable and well defined in the whole configuration space.

Yet, all aforementioned controllers share the same weakness: they all rely heavily on accurate knowledge of soft robot dynamic parameters, which is generally not available in the practice of soft robotics. In this letter, we tackle this challenge by adopting nonlinear adaptive control, built upon the technique pioneered by Li and Slotine in [12]. This framework has already been applied to articulated soft

This research was partly supported by the Science Fund of the Republic of Serbia, PROMIS, #6062528, ForNextCobot. ¹ Department of Engineering, University of Palermo, Italy, ² School of Electrical Engineering, University of Belgrade, Belgrade 11000, Serbia, ³ Department of Cognitive Robotics, Delft University of Technology (TU Delft), Delft, The Netherlands, ⁴ Institute of Robotics and Mechatronics, German Aerospace Center (DLR), Oberpfaffenhofen, Germany, ⁵ Department of Informatics, Technical University of Munich (TUM), Munich, Germany. Contacts maja.trumic@unipa.it, cosimodellasantina@gmail.com, kostaj@etf.rs, fagiolini@unipa.it.
978-1-6654-4197-1/\$31.00 ©2021 AACC

robots [13], [14], and to kinematic control of continuum soft robots [15]. Here, we tackle the substantially more challenging problem of dynamic control of continuum soft robots. In this respect, a second theoretical contribution is to show how to formulate the adaptive control calculations, and to describe the necessary and sufficient hypotheses for convergence. The contributions of this letter are the following: 1) a PCC-based model for a generic three-dimensional soft robot, ensuring kinematic and dynamic equivalence with the original system and having no representation singularities and discontinuities; 2) a robust closed-loop position controller for a soft-bodied robot, which is based on the nonlinear adaptive control theory; 3) extensive simulations - including piecewise constant curvature 3D and non-constant affine curvature soft robots - proving the effectiveness and the robustness of the controller.

II. A NEW PCC-BASED MODELING OF GENERIC SOFT-ROBOTS WITH IMPROVED PARAMETERIZATION

A. Background

Consider a soft-bodied robot consisting of n Constant-Curvature (CC) segments. Let $\{S_0\}$ be the robot's base frame and $\{S_1\}, \dots, \{S_n\}$ the n local frames attached to the end of each segment. Under the PCC assumption, i.e. when each segment can be characterized by a unique CC segment in the space, the i -th segment's configuration is fully determined by the frames $\{S_{i-1}\}$ and $\{S_i\}$. Accordingly, it suffices to adopt the following variables per segment [10]: 1) the angle ϕ_i between the bending plane and the plane described by the unit vectors \hat{n}_{i-1} and \hat{o}_{i-1} ; 2) the relative rotation θ_i between the two frames in the curvature plane; 3) the segment's length change δL_i , whose minimum is physically bounded by $-L_{0,i}$, where $L_{0,i} \in \mathbb{R}$ is the rest value. However, singularity issues arise whenever $\theta_i = 0$ or $\phi_i = \pm\pi$, which leads to known description inaccuracies.

It has been recently established that a singularity-free representation can be obtained by considering, for each segment, the four arcs originating from the positive and negative directions of the x and y axes of $\{S_{i-1}\}$ and terminating into the corresponding ones of $\{S_i\}$ [11]. Accordingly, the i -th segment configuration is $q_i = (\Delta_{x,i}, \Delta_{y,i}, \delta L_i)^T \in \mathbb{R}^3$ (see Fig. 2), where

$$\Delta_{x,i} = \frac{1}{2}(L_{2,i} - L_{1,i}), \text{ and } \Delta_{y,i} = \frac{1}{2}(L_{4,i} - L_{3,i}),$$

with $L_{j,i}$ being the four arc lengths ($j = 1, \dots, 4$). The two sets of coordinates are related by the invertible mapping

$$\phi_i = \arccos\left(\frac{\Delta_{x,i}}{\Delta_i}\right) = \arcsin\left(\frac{\Delta_{y,i}}{\Delta_i}\right), \quad \theta_i = \Delta_i/d_i, \quad (1)$$

where $\Delta_i = \sqrt{\Delta_{x,i}^2 + \Delta_{y,i}^2}$ and d_i is a free parameter, which can be chosen to match some specific location, e.g. where strain sensors are placed, so to have direct readings of the configuration. For the sake of space and readability, it is assumed $d_i = 1$ m in the remainder of the work. In terms of the elements of the configuration vector q_i , the i -th homogeneous transformation mapping S_{i-1} into S_i is $T_{i-1}^i = \begin{pmatrix} R_{i-1}^i & t_{i-1}^i \\ 0_{1 \times 3} & 1 \end{pmatrix}$, where R_{i-1}^i and t_{i-1}^i can be found in [11]. According to this notation, the configuration of a soft-bodied robot with n PCC segments is fully described by the vector $q = (q_1^T, \dots, q_n^T)^T \in \mathbb{R}^{3n}$.

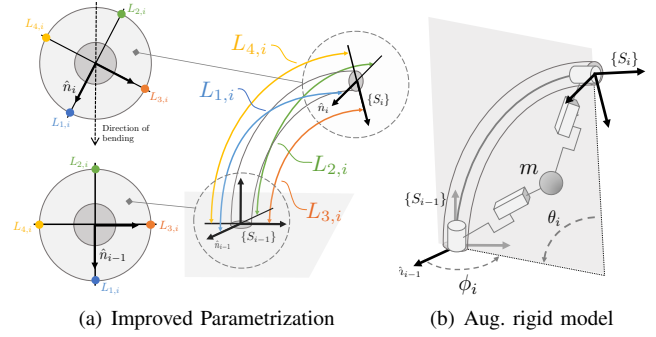


Fig. 2. Three dimensional description of a CC segment. Panel (a) shows the improved parameterization, which is free from singularities and discontinuities. We connect it to augmented rigid model in Panel (b).

B. Augmented PCC Representation with Improved Parameterization

Let us first focus on finding a globally-valid augmented representation for the i -th CC segment. The idea is that of trying to match the segment's kinematics and dynamic map with those of a classical rigid robot with sufficient degrees of freedom. The matching is obtained when the two models are said to be *kinematically* and *dynamically equivalent*, that is if the reference frame attached to the end-effector of the segment's augmented model coincides with that of the rigid robot, and when their respective centers of mass coincide, respectively. It has been shown very recently in [10] that an equivalent augmented representation can be obtained with a ten degree-of-freedom rigid robot whose segment variables are ϕ_i , θ_i , and δL_i . This model is almost always valid, except at the above-mentioned singularity configurations.

However, by leveraging on the recently developed improved parameterization [11], we proceed herein to a rigid-robot equivalent representation, using the variables $\Delta_{x,i}$, $\Delta_{y,i}$, and δL_i to describe each segment, for $i = 1, \dots, n$, which therefore has no singularity issues. In terms of the newly chosen configuration vector q_i , the augmented configuration vector $\xi_i \in \mathbb{R}^{10}$ from [11] can be described by a nonlinear map of the form $\xi_i = m_i(q_i) = m_i(\Delta_{x,i}, \Delta_{y,i}, \delta L_i)$, which explicitly reads:

$$\begin{pmatrix} \xi_{10(i-1)+1} \\ \xi_{10(i-1)+2} \\ \xi_{10(i-1)+3} \\ \xi_{10(i-1)+4} \\ \xi_{10(i-1)+5} \\ \xi_{10(i-1)+6} \\ \xi_{10(i-1)+7} \\ \xi_{10(i-1)+8} \\ \xi_{10(i-1)+9} \\ \xi_{10(i-1)+10} \end{pmatrix} = \begin{pmatrix} \arccos(\Delta_{x,i}/\Delta_i) \\ \frac{\Delta_i}{2} - \eta_i^*(q_i) \\ b_i^*(q_i) \\ \eta_i^*(q_i) \\ -\arccos(\Delta_{x,i}/\Delta_i) \\ \arccos(\Delta_{x,i}/\Delta_i) \\ \eta_i^*(q_i) \\ b_i^*(q_i) \\ \frac{\Delta_i}{2} - \eta_i^*(q_i) \\ -\arccos(\Delta_{x,i}/\Delta_i) \end{pmatrix}, \quad (2)$$

where $b_i^*(q_i) = \frac{L_{0,i} + \delta L_i}{\Delta_i} \gamma_i(q_i)$, $\eta_i^*(q_i) = \arccos(\sin(\frac{\Delta_i}{2})/\gamma_i(q_i))$, with $\gamma_i(q_i) = \sqrt{1 + \text{sinc}(\frac{\Delta_i}{2})(\text{sinc}(\frac{\Delta_i}{2}) - 2\cos(\frac{\Delta_i}{2}))}$, and the asterisk is used to distinguish them from the analogous ones in the previous ϕ_i , θ_i and δL_i based formalization. Recall that $\text{sinc}(x) = \sin(x)/x$ and its value in zero is 1.

Mapping m_i is globally defined as it holds

$$\lim_{\|q_i\| \rightarrow 0} b_i^*(q_i) = \frac{L_{0,i}}{2}, \quad \lim_{\|q_i\| \rightarrow 0} \eta_i^*(q_i) = 0, \\ \lim_{\|q_i\| \rightarrow 0} \arccos(\Delta_{x,i}/\Delta_i) = 0.$$

Following from the above reasoning, a globally-valid augmented representation of a soft-bodied robot, under the PCC hypothesis, can be obtained by serially connecting its n CC segments. This leads to an augmented vector $\xi \in \mathbb{R}^{10n}$ that is related to the robot's configuration $q = (\Delta_{x,1}, \Delta_{y,1}, \delta L_1, \dots, \Delta_{x,n}, \Delta_{y,n}, \delta L_n)^T$ via the decentralized mapping

$$\xi = m(q) = \begin{pmatrix} m_1(\Delta_{x,1}, \Delta_{y,1}, \delta L_1) \\ \vdots \\ m_n(\Delta_{x,n}, \Delta_{y,n}, \delta L_n) \end{pmatrix}. \quad (3)$$

Let us now move on to deriving the dynamic model corresponding to this new formalization. The rigid robot's dynamics described as a function of ξ reads

$$B_\xi(\xi) \ddot{\xi} + C_\xi(\xi, \dot{\xi}) \dot{\xi} + G_\xi(\xi) = \tau_\xi + J_\xi^T f_{\text{ext}}, \quad (4)$$

where $B_\xi, C_\xi \in \mathbb{R}^{10n \times 10n}$, $G_\xi \in \mathbb{R}^{10n}$ are the inertia and Coriolis matrices and gravity vector, respectively, $J_\xi \in \mathbb{R}^{6 \times 10n}$ the Jacobian of the direct kinematics, and τ_ξ and f_{ext} are the generalized forces along the ξ -coordinates and external wrench vector. Substituting in (4) the first two time derivatives of (3), i.e. the relations

$$\dot{\xi} = J_m(q) \dot{q}, \quad \ddot{\xi} = \dot{J}_m(q, \dot{q}) \dot{q} + J_m(q) \ddot{q}, \quad (5)$$

where $J_m(q) : \mathbb{R}^{3n} \rightarrow \mathbb{R}^{10n \times 3n}$ is the Jacobian of mapping $m(q)$ with respect to q , left-multiplying the resulting equation by J_m^T , and finally using (3) to replace ξ with q , we obtain the intermediate result:

$$B(q) \ddot{q} + C(q, \dot{q}) \dot{q} + G(q) = \tau^* + J^T(q) f_{\text{ext}},$$

where $B, C \in \mathbb{R}^{3n \times 3n}$, $G \in \mathbb{R}^{3n}$, $J(q) \in \mathbb{R}^{6 \times 3n}$ is the Jacobian of the direct kinematics with respect to q , and $\tau^* = (\tau_{x,1}^*, \tau_{y,1}^*, \tau_{L,1}^*, \dots, \tau_{x,n}^*, \tau_{y,n}^*, \tau_{L,n}^*)^T$ is the generalized force along the q -coordinates. Specifically, we have:

$$B(q) = J_m^T B_\xi(m(q)) J_m,$$

$$C(q, \dot{q}) = J_m^T (B_\xi(m(q)) \dot{J}_m + C_\xi(m(q), J_m \dot{q}) J_m),$$

$$G(q) = J_m^T G_\xi(m(q)), \quad J(q) = J_\xi(m(q)) J_m.$$

As a further step, we can now add at segment level [11] the elastic and friction terms, which are proportional to q and \dot{q} , respectively, and thus can be described via a block-diagonal stiffness matrix $K = \text{diag}(K_1, \dots, K_n)$, with $K_i = \text{diag}(k_{\Delta_{x,i}}, k_{\Delta_{y,i}}, k_{\delta L_i})$, and a block-diagonal damping matrix $D = \text{diag}(D_1, \dots, D_n)$, with $D_i = \text{diag}(\beta_{\Delta_{x,i}}, \beta_{\Delta_{y,i}}, \beta_{\delta L_i})$. Finally, to complete the model, we can express the i -th segment's subset of inputs, $\tau_{x,i}^*$, $\tau_{y,i}^*$, and $\tau_{L,i}^*$, as linear combinations of the corresponding externally applicable inputs, $\tau_{x,i}$, $\tau_{y,i}$, and $\tau_{L,i}$, via the segment's actuation sub-matrix

$$A_i = \begin{pmatrix} \frac{\Delta_{x,i} \Delta_{y,i}}{\Delta_i^2} \nu_i & -\frac{\Delta_{x,i}^2 \nu_i + \Delta_i^2 \sin \Delta_i}{\Delta_i^2} & \frac{\Delta_{x,i} \nu_i}{\Delta_i^2} L_i \\ \frac{\Delta_{y,i}^2 \nu_i + \Delta_i^2 \sin \Delta_i}{\Delta_i^2} & -\frac{\Delta_{x,i} \Delta_{y,i}}{\Delta_i^2} \nu_i & \frac{\Delta_{y,i} \nu_i}{\Delta_i^2} L_i \\ 0 & 0 & \text{sinc}(\Delta_i) \end{pmatrix}.$$

with $\nu_i = 1 - \text{sinc}(\Delta_i)$ and $L_i = L_{0,i} + \delta L_i$. The robot's overall actuation matrix is therefore given by $A(q) = \text{diag}(A_1(q_1), \dots, A_n(q_n))$, where each A_i is globally well-defined. Moreover, since each A_i 's determinant is $\text{sinc}^2(\Delta_i)$, the robot remains fully actuated except at configurations with $\Delta_i = \mu \pi$, with $\mu \in \mathbb{N}$, for some i . In conclusion, the sought soft-bodied robot's dynamics can be written as

$$B(q) \ddot{q} + C(q, \dot{q}) \dot{q} + G(q) + K q + D \dot{q} = A \tau + J^T f_{\text{ext}}, \quad (6)$$

where $\tau = (\tau_{x,1}, \tau_{y,1}, \tau_{L,1}, \dots, \tau_{x,n}, \tau_{y,n}, \tau_{L,n})^T$. Without loss of generality, the external wrench vector is assumed null, i.e. $f_{\text{ext}} = 0$, in the remainder of the paper.

Before concluding, we point out that the augmented formulation yields properties facilitating the application of classical control approaches. For the sake of space, we only report here their statements as their proofs follow from [9].

Proposition 1. *The inertia matrix $B(q)$ is positive semi-definite and bounded, i.e. $B(q) \succeq 0$, $\|B(q)\| < \infty, \forall q \in \mathbb{R}^n$, if $\|J_m\| < 1$ and $|m_i(q)| < \infty$ for all $q \in \mathbb{R}^n$ and $\forall i$ such that the i -th joint is prismatic. Moreover, under the above hypothesis on B , given any matrix $R(q) \in \mathbb{R}^{n \times d_r}$ such that $\text{rank}(B_\xi(m(q))) = d_r$ and $\text{span}(R(q))$ is the range of $B_\xi(m(q))$, then $\text{rank}(R^T J_m(q)) = n$ implies that $B(q) \succ 0$.*

Proposition 2. *If $C_\xi(\xi, \dot{\xi})$ is obtained via Christoffel symbols, then matrix $\dot{B}(q) - 2C(q, \dot{q})$ is skew-symmetric. If C_ξ is not built through Christoffel symbols, then $\dot{q}^T (\dot{B}(q) - 2C(q, \dot{q})) \dot{q} = 0$.*

This formalization enables modeling of soft-bodied robots as fully-actuated rigid ones, with no singularities, thus providing an easier and standard strategy for the derivation of stability proof theorems, as it has been already evidenced in [9], where a computed torque and Cartesian impedance control are developed. It also allows capitalizing on classical robust control techniques, as we do in the following.

III. ADAPTIVE CONTROL OF SOFT-BODIED ROBOTS

Adaptive control is a technique robust to model uncertainties due to imprecise knowledge of system parameters [12]. It ensures the asymptotic tracking of desired joint trajectories via dynamic adaptation of a set of parameters. The method's applicability relies on the dynamics' linearity with respect to suitable parameters, i.e. the ability to write it as the product of a regressor matrix Y and a constant parameter vector π . In its basic formulation, it also requires a full actuation.

We first show that the linearity property is preserved in our newly proposed model. As the dynamics in (4) is that of a standard rigid robot, it is linear with respect to a parameter vector π_ξ , i.e. we have $Y_\xi(\xi, \dot{\xi}, \ddot{\xi}) \pi_\xi = \tau_\xi$, for some matrix Y_ξ . This implies that analogous decompositions hold for each addend appearing in (4): $B_\xi(\xi) \ddot{\xi} = Y_{B_\xi}(\xi, \dot{\xi}) \pi_{B_\xi}$, $C_\xi(\xi, \dot{\xi}) \dot{\xi} = Y_{C_\xi}(\xi, \dot{\xi}) \pi_{C_\xi}$, and $G_\xi(\xi) = Y_{G_\xi}(\xi) \pi_{G_\xi}$. We can also observe that $m(q)$ linearly depends on $L_{0,i}$ and thus it holds $J_m(q) = Y_m(q) \pi_m$ for suitable Y_m and π_m . Moreover, the left hand-side of (6) can be easily written as

$$J_m^T B_\xi(m(q)) \ddot{\xi} + J_m^T C_\xi(\xi, \dot{\xi}) \dot{\xi} + J_m^T G_\xi(\xi) + K q + D \dot{q}.$$

Its first addend can be factorized as follows:

$$\begin{aligned} J_m^T B_\xi(m(q)) \ddot{\xi} &= \pi_m^T Y_m^T Y_{B_\xi}(\xi, \ddot{\xi}) \pi_{B_\xi} = \\ &= \pi_m^T Y_m^T Y_{B_\xi}(m(q), \dot{J}_m \dot{q} + J_m \ddot{q}) \pi_{B_\xi}, \end{aligned}$$

where (3) and (5) have been used. By using similar reasoning as in Property 2 from [16], we can find suitable Y_B and π_B such that $J_m^T B_\xi(m(q)) \ddot{\xi} = Y_B(q, \dot{q}, \ddot{q}) \pi_B$. With similar steps, the second and third addends can be written as follows:

$$\begin{aligned} J_m^T C(\xi, \dot{\xi}) \dot{\xi} &= \pi_m^T Y_m^T Y_{C_\xi}(m(q), \dot{J}_m \dot{q} + J_m \ddot{q}) \pi_{C_\xi} = \\ &= Y_C(q, \dot{q}) \pi_C, \\ J_m^T G(\xi) &= \pi_m^T Y_m^T Y_{G_\xi}(\xi) \pi_{G_\xi} = \\ &= J_m^T Y_{G_\xi}(m(q)) \pi_{G_\xi} = Y_G(q) \pi_G. \end{aligned}$$

Decomposing also $Kq = Y_K(q) \pi_K$ and $D\dot{q} = Y_D(\dot{q}) \pi_D$, and summing up the three addends above yields:

$$Y(q, \dot{q}, \ddot{q}) \pi = A(q) \tau, \quad (7)$$

with regressor matrix $Y = (Y_B, Y_C, Y_G, Y_K, Y_D)$ and parameter vector $\pi = (\pi_B^T, \pi_C^T, \pi_G^T, \pi_K^T, \pi_D^T)^T$.

Leveraging on Prop. 1 and 2, we are now ready to derive the following result:

Theorem 1 (Adaptive Controller). *Given a soft-bodied robot as in (6), the dynamic control law*

$$\begin{aligned} \dot{\hat{\pi}} &= K_\pi Y^T(q, \dot{q}, \dot{q}_r, \ddot{q}_r) \sigma, \\ \tau &= A(q)^\dagger (Y(q, \dot{q}, \dot{q}_r, \ddot{q}_r) \hat{\pi} + K_d \sigma), \end{aligned}$$

where $\hat{\pi}$ is the parameter estimate vector, $\dot{q}_r = \dot{q}_d + \Lambda(q_d - q)$, $\sigma = \dot{q}_d - \dot{q} + \Lambda(q_d - q)$, K_π , Λ and K_d are free positive definite matrices, and $A(q)^\dagger$ is the pseudo-inverse of $A(q)$, ensures asymptotic tracking of any desired trajectory vector signal $q_d(t) \in \mathcal{C}^2$.

Proof. In order to apply the adaptive approach proposed in [12], which avoids using the second time-derivative of q , we first introduce the reference speed \dot{q}_r and rewrite the robot's dynamics as

$$B(q) \ddot{q}_r + C(q, \dot{q}) \dot{q}_r + G(q) + Kq + D\dot{q} = A(q) \tau.$$

By exploiting the linearity property shown in (7), we can write the left hand-side of the above expression as the product of a regressor matrix $Y(q, \dot{q}, \dot{q}_r, \ddot{q}_r)$ and the corresponding parameter vector π .

Additionally, we can define a new input $\tau^* = A(q) \tau$. Being $A(q)$ exactly known (and indeed independent of any robot's parameters) and also invertible, except at isolated points, the adaptive control law described in [12] can be applied via τ^* , and then translated back to τ by using the pseudo-inverse of $A(q)$, i.e. as $\tau = A(q)^\dagger \tau^*$. The rest of the proof straightforwardly follows from [12]. \square

In a realistic scenario, position and speed information for all configurations can be obtained via commercial motion-capture systems, embedded proprioceptive sensors, or a combination of them [17]. In such approaches, the kinematic map from [11] has been adopted. Though not being based on the augmented formulation, it provides an equivalent information from the sensing viewpoint.

IV. SIMULATIONS

The performance and robustness of our control method are validated here under the presence of measurement noise, external disturbance, and initial tracking error. Three setups have been considered: a planar soft-bodied robot modeled with the PCC approximation, a soft inverted pendulum with affine non-constant curvature, and a 3D soft robot. The recursive Newton-Euler formulation provided by Peter Corke's Robotics Toolbox is used to efficiently compute B_ξ , C_ξ , G_ξ , and J_ξ in Eq. 4. All robot parameters including mass, length, stiffness, and damping of each segment are assumed to be fully unknown, and thus the initial values of the estimated parameter vector $\hat{\pi}$ are set to be null in all simulations.

1) *Planar Soft Manipulator*: As a first case, we consider a planar soft robot composed of four independently-actuated and equal segments with length $L = 0.1$ m, mass $m = 10$ g, stiffness $k = 1$ Nm/rad, and damping $\beta = 0.1$ Nm·s/rad. The robot's base frame is chosen so that its tip points downwards and is aligned with gravity when all joint angles are null. To ensure kinematics and dynamic equivalence on the plane, each segment is modeled as a four-DoF rigid robot according to the augmented formulation presented in [9]. Since the PCC-based planar formulation has no singularity and discontinuity issues, we can use here the bending angle θ_i as a configuration variable. The controller uses a regressor matrix $Y \in \mathbb{R}^{4 \times 173}$ built on such a model, with an initial parameter vector value of $\hat{\pi}(0) = 0_{173}$. In Fig. 3, we present the results obtained when the robot is required to track the reference signals $\theta_{d,i} = M_i \sin(\omega t + \varphi_i)$, with $\omega = 1$ rad/s and M_i and φ_i being the i -th entries of the vectors $M = (\frac{\pi}{8}, \frac{\pi}{6}, \frac{\pi}{3}, \frac{\pi}{2})$ rad and $\varphi = (0, \frac{\pi}{2}, \frac{\pi}{3}, \pi)$ rad, respectively. The figure illustrates the results obtained with lower and higher control gains starting from an initial tracking error of $(1, -1, 1, -1)^T$ rad.

2) *Soft inverted pendulum with affine curvature*: Consider a continuum soft robot behaving as a soft inverted pendulum under the effect of gravity [18]. Let $L = 1$ m, $m = 1$ kg, $k = 1$ Nm/rad, and $\beta = 0.1$ Nm·s/rad be its length, mass, stiffness, and damping, respectively. Having defined the system's configuration vector as $\theta = (\theta_0, \theta_1)^T$, the instantaneous robot's shape can be described by the affine curvature $\kappa_s(t, s) = \theta_0(t) + \theta_1(t)s$, where $s \in [0, 1]$ parameterizes the position along the main axis of the pendulum, in such a way that Ls is the arc length of the path connecting the base to the point s through the main axis. The soft pendulum's dynamics can then be modeled as $B(\theta) \ddot{\theta} + C(\theta, \dot{\theta}) \dot{\theta} + G(\theta) + k H \theta + \beta H \dot{\theta} = H[1 \ 0]^T \tau$, with $B(\cdot)$, $C(\cdot)$, and $G(\cdot)$ being derived by appropriately summing up the infinitesimal mass elements [18], $H \in \mathbb{R}^{2 \times 2}$ with $H_{i,j} = 1/(i+j-1)$ is the Hankel matrix. It is notable that this model generalizes the PCC-based one described in Sec. II, for which it stands $\theta_0 \equiv 0$. Constructing the regressor matrix Y according to Sec. III, for the case of a planar single segment, yields $Y(\theta_0, \dot{\theta}_0, \ddot{\theta}_{0,r}, \ddot{\theta}_{0,r}) = (y_1, y_2, \theta_0, \dot{\theta}_{0,r})$, with

$$\begin{aligned} y_1 &= \frac{\ddot{\theta}_{0,r}}{16} \left((\text{sinc}'(\frac{\theta_0}{2}))^2 + 4 \text{sinc}^2(\frac{\theta_0}{2}) + 16 \right) + \\ &\quad + \frac{\dot{\theta}_{0,r} \ddot{\theta}_0}{16} \text{sinc}'(\frac{\theta_0}{2}) (\text{sinc}''(\frac{\theta_0}{2}) + 2 \text{sinc}(\frac{\theta_0}{2})), \\ y_2 &= -\frac{1}{4} (2 \text{sinc}(\frac{\theta_0}{2}) \cos(\frac{\theta_0}{2}) + \text{sinc}'(\frac{\theta_0}{2}) \sin(\frac{\theta_0}{2})), \end{aligned}$$

and to a parameter vector $\pi = (mL^2, mgL, k, \beta)^T$. Fig. 4 illustrates the results obtained with a soft inverted pendulum with low stiffness ($k = 1$ Nm/rad) and one with medium

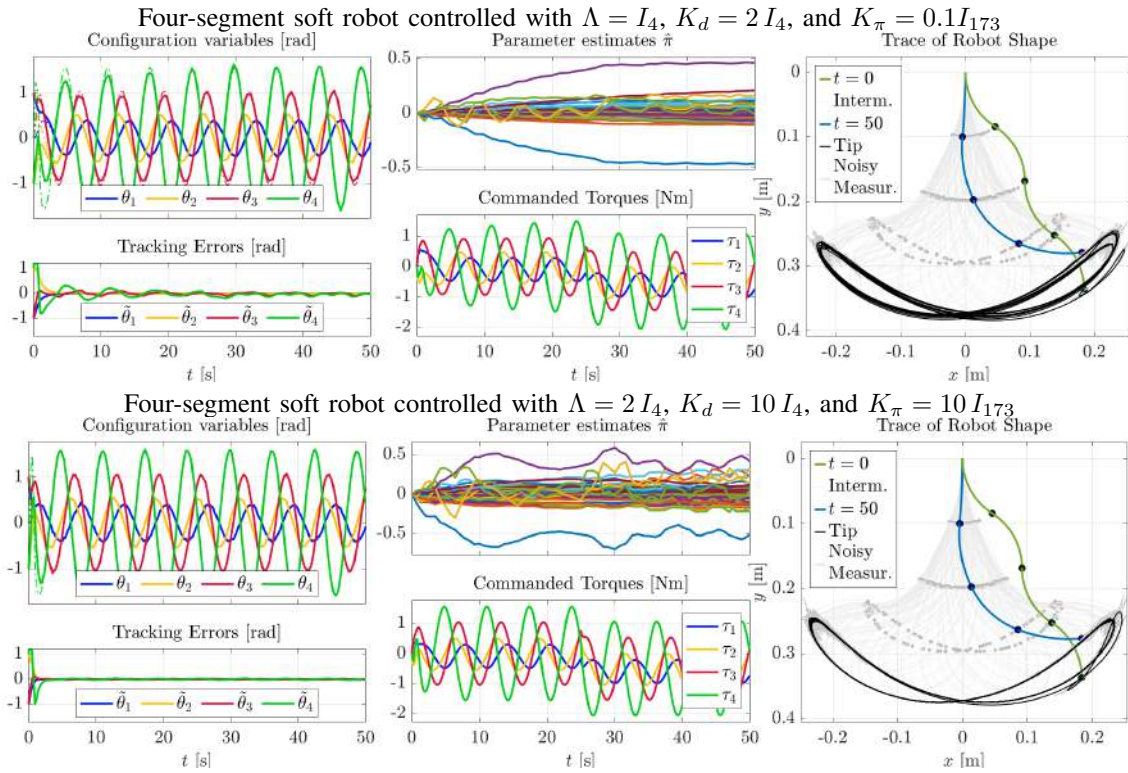


Fig. 3. Scenario #1: The two rows report, from left to right, the configuration variable evolution (dashed lines indicate the desired trajectories) and the corresponding tracking errors $\tilde{\theta}_i = \theta_{i,d} - \theta_i$, the estimated parameters and commanded torques, and a trace of the robot's shape. A persistent constant force of 0.5 N is applied from $t = 25$ s on each segment, simulating an external disturbance. The measurement of each configuration variable is affected by Gaussian white noise with zero mean value and standard deviation of 0.032 rad. As expected from theory, higher control gains allow a faster tracking convergence and a more precise tracking since the beginning. It can be noticed that the parameter estimates nicely behave and remain bounded. The approach is robust also to the presence of external disturbance and measurement noise.

stiffness ($k = 4$ Nm/rad); the former is regulated to the upright position by a controller with gains $\Lambda = 0.2$, $K_d = 0.05$, and $K_\pi = 0.01 I_4$, and the latter by one with gains $\Lambda = 0.1$, $K_d = 0.1$, and $K_\pi = 0.05 I_4$. In both cases the initial tracking error is $(\pi/4, -\pi/4)^T$ rad. It should be noted that the small value of the external disturbance is only chosen so as to keep the response times of both pendulums short, while a bigger value would lead to a longer settling time but would be successfully handled by the approach.

3) *Soft Manipulator in 3D space*: We finally consider a generic soft-bodied robot composed of four CC segments in a 3D space whose model is described by Eq. 6. The four segments are assumed to be identical and characterized by $L_{i,0} = 1$ m, $m_i = 1$ kg, $k_i = 1$ Nm/rad, $\beta_i = 0.1$ Nms/rad, for $i = \{1, 2, 3, 4\}$. Deriving and using an adaptive controller based on such a model is challenging due to the large number of involved functions and parameters. We proceed therefore by building it based on the simplified model presented in [11]. The desired reference signals for both segments are sinusoidal, the controller gains are $\Lambda = 7 I_{12}$, $K_d = 13 I_{12}$, and $K_\pi = 2 I_{60}$, the regressor matrix is $Y \in \mathbb{R}^{12 \times 60}$, and the initial parameter vector is $\hat{\pi}(0) = 0_{60}$. The obtained results are shown in Fig. 5, where the initial tracking error is 0.05 m for each of the three configuration variables of the first two segments, and -0.05 m for those of the other two.

V. CONCLUSION

This letter presented a novel solution for the control of soft-bodied robot position. Based on the nonlinear adaptive

control theory, the approach enables a successful tracking performance even when significant parametric uncertainties exist. Validation of the method has been carried out on various robot configurations, thus proving also its robustness. A still open question connected to the applicability of the proposed method is connected to the maximum number of segments used to represent a given soft-bodied robot. To this respect, thanks to the dynamic equivalence herein established, our work can benefit from studies seeking for the minimum information required for an adaptive controller to accurately regulate a soft-robot [16]. It should also be noticed that the regressor is evaluated off-line and once before the actual control action is executed. The results presented in this work show the ability of our method to reject external disturbance and cope with measurement noise. Future work will be devoted to testing the algorithm with real experiments, where the state space is truly infinite dimensional, and extending it to black box uncertainties.

REFERENCES

- [1] D. Rus and M. T. Tolley, "Design, fabrication and control of soft robots," *Nature*, vol. 521, no. 7553, pp. 467–475, 2015.
- [2] T. G. Thuruthel, E. Falotico, M. Manti, and C. Laschi, "Stable open loop control of soft robotic manipulators," *IEEE Robot. Autom. Lett.*, vol. 3, no. 2, pp. 1292–1298, 2018.
- [3] A. Mironchenko and C. Prieur, "Input-to-state stability of infinite-dimensional systems: recent results and open questions," *SIAM Review*, vol. 62, no. 3, pp. 529–614, 2020.
- [4] S. Grazioso, G. Di Gironimo, and B. Siciliano, "A geometrically exact model for soft continuum robots: The finite element deformation space formulation," *Soft robotics*, vol. 6, no. 6, pp. 790–811, 2019.

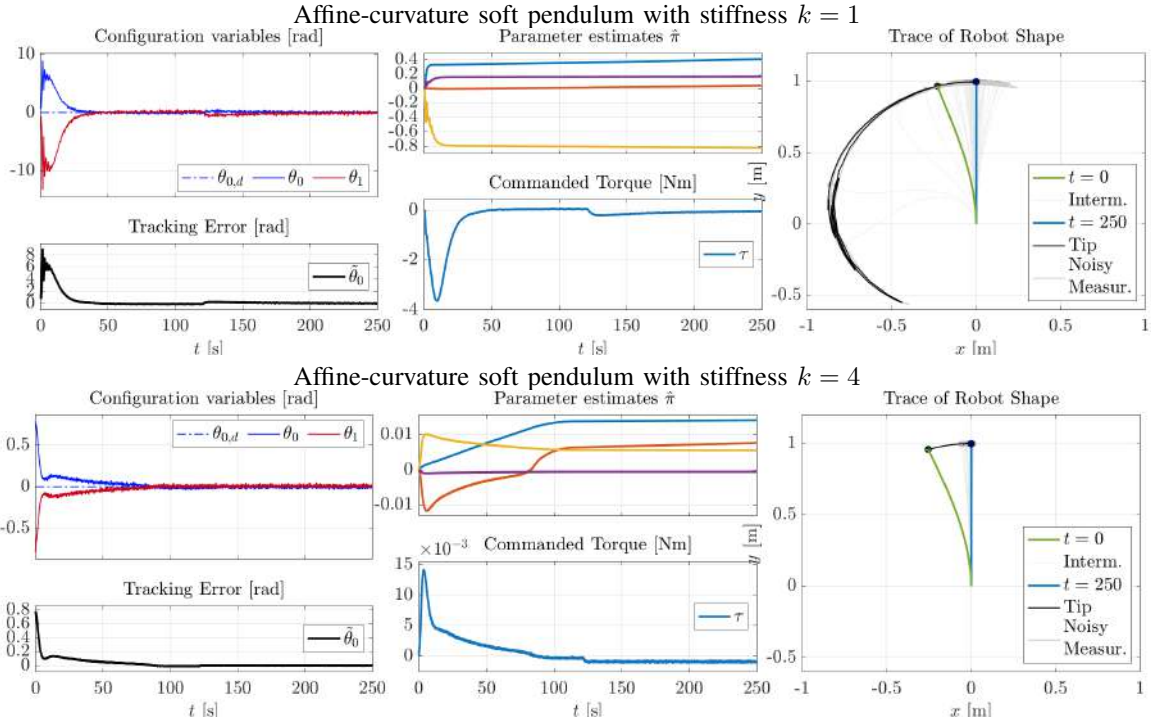


Fig. 4. Scenario #2: Affine-curvature soft pendulum subject to gravity. The proposed controller allows asymptotically stabilizing the robot to the upright position both with a lower and a higher stiffness. The standard deviation of the measurement noise is 0.032 rad, and a persistent constant disturbance of $5 \cdot 10^{-3}$ N is applied from $t = 125$ s.

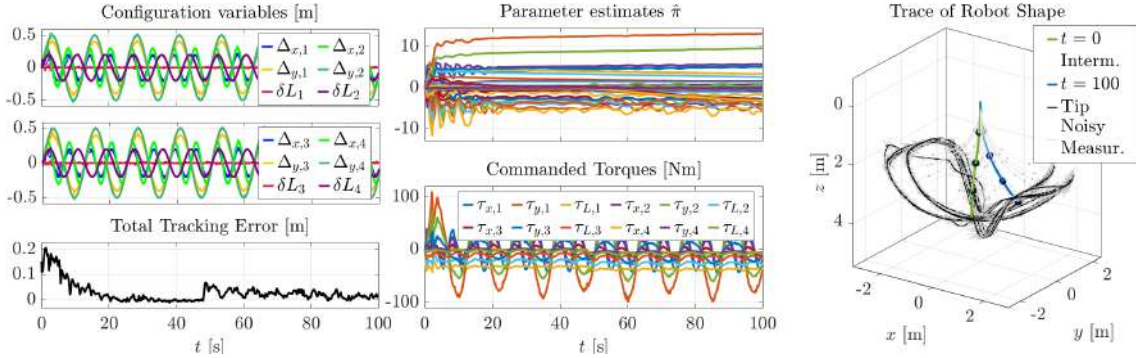


Fig. 5. Scenario #3: Four-segment 3D soft-bodied robot tracking sinusoidal references. A Gaussian white noise with zero mean value and standard deviation of 0.032 m affects all configuration measures, and a persistent constant force of amplitude 5 N is applied on each segment from $t = 50$ s. The total tracking error is computed as the 2-norm of the vector composed of the tracking errors along all components. The simulation shows the controller's ability to adapt the parameter estimates, even with noise and disturbances, so as to track the desired signals.

- [5] S. H. Sadati, S. E. Naghibi, A. Shiva, B. Michael, L. Renson, M. Howard, C. D. Rucker, K. Althoefer, T. Nanayakkara, S. Zschaler *et al.*, "Tmtdyn: A matlab package for modeling and control of hybrid rigid-continuum robots based on discretized lumped systems and reduced-order models," *SAGE The Intl. J. Robot. Res.*, pp. 1–52, 2019.
- [6] M. Thieffry, A. Kruszewski, C. Duriez, and T.-M. Guerra, "Control design for soft robots based on reduced-order model," *IEEE Robot. Autom. Lett.*, vol. 4, no. 1, pp. 25–32, 2018.
- [7] R. J. Webster III and B. A. Jones, "Design and kinematic modeling of constant curvature continuum robots: A review," *SAGE The Intl. J. of Robot. Res.*, vol. 29, no. 13, pp. 1661–1683, 2010.
- [8] V. Falkenhahn, A. Hildebrandt, R. Neumann, and O. Sawodny, "Model-based feedforward position control of constant curvature continuum robots using feedback linearization," in *2015 Intl. Conf. Robot. Autom. IEEE*, 2015, pp. 762–767.
- [9] C. Della Santina, R. K. Katzschmann, A. Bicchi, and D. Rus, "Model-based dynamic feedback control of a planar soft robot: Trajectory tracking and interaction with the environment," *SAGE The Intl. J. Robot. Res.*, vol. 39, no. 4, pp. 490–513, 2020.
- [10] R. K. Katzschmann, C. Della Santina, Y. Toshimitsu, A. Bicchi, and D. Rus, "Dynamic motion control of multi-segment soft robots using piecewise constant curvature matched with an augmented rigid body model," in *2nd Intl. Conf. Soft Robot. IEEE*, 2019, pp. 454–461.
- [11] C. Della Santina, A. Bicchi, and D. Rus, "On an improved state parametrization for soft robots with piecewise constant curvature and its use in model based control," *IEEE Robot. Autom. Lett.*, vol. 5, no. 2, pp. 1001–1008, 2020.
- [12] J.-J. E. Slotine, W. Li *et al.*, *Applied nonlinear control*. Prentice hall Englewood Cliffs, NJ, 1991, vol. 199, no. 1.
- [13] G. Tonietti and A. Bicchi, "Adaptive simultaneous position and stiffness control for a soft robot arm," in *Intl. Conf. Intelligent Robots and Systems*, vol. 2. IEEE/RSJ, 2002, pp. 1992–1997.
- [14] M. Trumić, K. Jovanović, and A. Fagiolini, "Decoupled nonlinear adaptive control of position and stiffness for pneumatic soft robots," *SAGE The Intl. J. Robot. Res.*, pp. 1–19, 2020.
- [15] H. Wang, B. Yang, Y. Liu, W. Chen, X. Liang, and R. Pfeifer, "Visual servoing of soft robot manipulator in constrained environments with an adaptive controller," *Trans. Mech.*, vol. 22, no. 1, pp. 41–50, 2016.
- [16] T. Marcucci, C. Della Santina, M. Gabiccini, and A. Bicchi, "Towards minimum-information adaptive controllers for robot manipulators," in *2017 Amer. Control Conf. IEEE*, 2017, pp. 4209–4214.
- [17] C. Della Santina, R. L. Truby, and D. Rus, "Data-driven disturbance observers for estimating external forces on soft robots," *IEEE Robot. Autom. Lett.*, vol. 5, no. 4, pp. 5717–5724, 2020.
- [18] C. Della Santina, "Soft inverted pendulum with affine curvature," in *2020 Conference on Decision and Control. IEEE*, 2020, pp. 1–8.